Am J Cancer Res 2021;11(12):5933-5950
www.ajcr.us /ISSN:2156-6976/ajcr0137838

Original Article

A Notch inhibitor plus Resveratrol induced blockade of autophagy drives glioblastoma cell death by promoting a switch to apoptosis

Francesca Giordano[1*], Francesca Ida Montalto[1,2*], Maria Luisa Panno[1], Sebastiano Andò[1,2#], Francesca De Amicis[1,2#]

[1]Department of Pharmacy, Health and Nutritional Sciences, University of Calabria, Italy; [2]Health Center, University of Calabria, Italy. [*]Co-first authors. [#]Co-senior authors.

Received July 30, 2021; Accepted October 23, 2021; Epub December 15, 2021; Published December 30, 2021

Abstract: Glioblastoma multiforme (GBM) is the most common and aggressive form of brain tumors and the hardest type of cancer to treat. Therapies targeting developmental pathways, such as Notch, eliminate neoplastic glioma cells, but their efficacy can be limited by various mechanisms. Combination regimens may represent a good opportunity for effective therapies with durable effects. We used low doses of the γ-secretase inhibitor RO4929097 (GSI), to block the Notch pathway activity, in combination with Resveratrol (RSV) and we evidenced the mechanisms of autophagy/apoptosis transition in GBM cells. Resveratrol and GSI combination results in the synergistic induction of cell death together with the block of the autophagic flux evidenced by a sustained increase of LC3-II and p62 protein content, due to the dramatic reduction of CDK4, an important regulator of lysosomal function. The ectopic overexpression of the constitutive active CDK4 mutant, greatly counteracted the RSV+GSI induced block of the autophagy. Triggering autophagy in RSV+GSI-treated cells, which have impaired lysosomal function, caused the collapse of the system and a following apoptosis. For instance, by combining the CDK4 mutant as well as the early stage autophagy inhibitor, 3-methyladenina, abolished the RSV+GSI induced caspases activation. The initiator caspases (caspases-8 and -9), effector caspase (caspase-3) and its downstream substrate PARP were induced after RSV+GSI exposure as well as the percentage of the TUNEL positive cells. Moreover, the pro-apoptotic signaling MAPK p38 was activated while the pro-survival MAPK p42/p44 signaling was inhibited. In short, we establish the role of CDK4 in the regulation of autophagy/apoptosis transition induced by RSV and GSI in GBM cells. This new synergistic therapeutic combination, increasing the accumulation of autophagosomes, may have therapeutic value for GBM patients.

Keywords: cdk4, cell death, Atg12, brain, cancer, gamma secretase inhibitor

Introduction

Glioblastoma multiforme (GBM) is the most common primary brain tumor in adults and unfortunately, the most aggressive and lethal form. The mean survival is only 12/15 months after diagnosis and in patients who receive the standard treatment of resection, radiation therapy and chemotherapy, the mean 5-year survival is <5% [1]. The challenge is therefore to discover new targets and develop new treatments to ameliorate the survival and quality of life for GBM patients. The majority of clinical trial approaches target the oncogenic signaling acting through tyrosine receptor kinases [2, 3], although also a variety of amplification cascades, including the RAS/RAF/MAPK and the PI3K/AKT/mTOR pathways are known to play important and decisive roles in GBM initiation and progression [4]. Additionally, aberrant Notch signaling is linked to the pathogenesis of brain tumors, even though the components are rarely mutated [5, 6].

In mammals four isoforms of the Notch receptor (Notch 1/2/3/4) are described [7]. Each Notch receptor is a single pass transmembrane protein with an intracellular domain (NCDI) and an extracellular domain (NECD). Upon ligand receptor binding, the Notch receptor undergoes proteolytic cleavage, by metalloprotease and gamma-secretase, thus the NCID can translo-

cate in the nucleus activating target genes transcription. The Notch pathway controls differentiation, proliferation, apoptosis, cell survival. The activation of Notch signaling confers a growth advantage by keeping tumor cells in a stem cell-like proliferative state and it is reported that pharmacological Notch blockade can induce protective autophagy in glioma neurospheres [8].

Given its significant role in tumor biology, the Notch pathway has been targeted *in vivo,* using antibodies and a range of inhibitors, counting small-molecule inhibitors as well as gamma-secretase inhibitors [9]. Particularly, a gamma-secretase inhibitor, RO4929097 (GSI) is an orally bioavailable small-molecule, capable of a potent, inhibitory effect on Notch signaling [10]. It has been tested in early-phase trials also in combination with other agents [11, 12], with responses detected in a variety of tumor types [12]. Very recently, in a phase II and pharmacodynamic trial for patients with recurrent/progressive GBM, GSI demonstrated minimal inhibition of neurosphere formation in fresh tissue samples [13]. In a phase 0/I trial, GSI was added to chemoradiotherapy for GBM treatment [11]. A comprehensive integrated translational approach demonstrated encouraging effectiveness, however also evidenced that glioma stem cell populations adapt to alterations in the microenvironment, thereby switching to a Notch-independent form of angiogenesis [14]. Besides, gamma-secretase inhibitors fail to distinguish individual Notch receptors, inhibit other signaling pathways, cause severe intestinal toxicity [15] and arrested cell proliferation in the intestinal crypts. For all these reasons the clinical application of gamma-secretase inhibitors is increasingly restricted.

The rational design of combination regimens may represent a good opportunity for effective therapies with durable effects in GBM patients. For instance, agents able to act on various targets exerting marginal toxicity would be potential additional drugs to the existing therapeutic portfolio. In this concern, Resveratrol (RSV; 3,5,40-trihydroxy-trans-stilbene), a phytoalexin present in grapes, is able of antiproliferative and protective action against various types of cancers [16-18]. The RSV effects involve the modulation of a huge number of molecular targets and signaling pathways [19], including JAK/STAT, Notch [20], NF-κB/p50/p65 and p53 pathways, to induce cell cycle arrest, apoptosis and autophagy in various types of tumor cells [17, 21, 22]. Specifically, in GBM cell lines, SHG44 and T98G, RSV potentiates the toxicity of temozolomide (TMZ) [23, 24], even though it has been found that human GBM cell lines respond differently to RSV [25]. Interestingly, over the last decades, RSV has received considerable attention due to its ability to cross the blood brain barrier [19].

In the present study we show that RSV, as a combination with GSI results in the synergistic induction of apoptotic cell death in GBM cell lines. We found that RSV+GSI serves as autophagy initiation inducer and also novel autophagic flux inhibitor, by interfering with autophagosome-lysosome fusion. In addition, the induced autophagosome accumulation is required for RSV+GSI-induced cell death. We demonstrated that the autophagic block and apoptosis are crucially related to CDK4 inhibition. Our study proposes a novel and significant therapeutic approach in which the combination with RSV enhances the efficacy of GSI, suggesting a strategy to reduce its side effects.

Materials and methods

Reagents

RO4929097 (GSI), Resveratrol (Rsv), aprotinin, leupeptin, phenylmethylsulfonyl fluoride (PMFS), sodium orthovanadate, NaCl, $MgCl_2$, EGTA, glycerol, Triton X-100, HEPES from Sigma-Aldrich (Milano, Italy). 3 Methil Adenine and Bafilomicin were from Merck Spa, (Milano, Italy) were dissolved as recommended by the manufacturer. Antibodies used in this study: anti-Notch 1, anti-cleaved Notch 1 (NICD), anti-HES 1, anti-HEY 1, anti-LC3B, anti-SQSTM1/p62, anti-Beclin-1, anti-pMAPK 38, anti-MAPK 38, anti-pMAPK44/42, anti-MAPK 44/42, anti-caspase-9, anti-caspase-8, anti-caspase-3 and anti-Bad were acquired from Cell Signaling Technology (Danvers, MA, USA); human anti-β-actin (SC-69879), anti-p27 (SC-53871), anti-cyclin E (SC-247), anti-p21 (SC-6246), anti-cyclinB1 (SC-245), anti-p53 (SC-126), anti-cyclin D1 (SC-8396), anti-Cdk4 (SC-23896), anti-Bcl2 (SC-7382), anti-ATG12 (SC-68884) anti-PARP1 (SC-7150) and Protein A/G PLUS-Agarose were from Santa Cruz Biotechnology (Dallas, TX, USA).

Plasmids

CDK4R24C expression vector (Plasmid #111-29) was from Addgene, GFP-LC3 Expression Vector (#CBA-401) was from Cell Biolabs, Inc. (San Diego, CA).

Cell culture

Human fetal glial cells SVG p12, human glioblastoma cell lines U87MG and T98G and human breast cancer cells T47D, were purchased from ATCC (Manassas, VA, USA). The SVG p12, U87MG and T98G cells were cultured in Minimum Essential Medium (Life Technologies, Monza MB, Italy), including 10% heat-inactivated fetal bovine serum (FBS), 200 mM L-glutamine, 1% penicillin-streptomycin, 1% Eagle's nonessential amino acids, and 1% sodium pyruvate (Sigma Aldrich). T47D cells were maintained as reported previously [49]. Cells were cultured at 37°C in a humidified atmosphere with 5% carbon dioxide. Cells were stored following the supplier's recommendations, and authenticated every six months after frozen aliquot resuscitations and regularly tested for mycoplasma negativity (MycoAlert Mycoplasma Detection Assay, Lonza, Basilea, CH, Switzerland).

MTT assay

The 3-(4,5-Dimethylthiazol-2-yl)-2,5-diphenyltetrazolium bromide (MTT, #M5655 Sigma Aldrich, Milan, Italy) assay was performed as previously reported [50]. Cells were plated in 96-well plates and treated as indicated. 50 µl of MTT stock solution (5 mg/ml in PBS) was added to each well and incubated at 37°C for 2 hours. The media was removed and 100 µl of dimethyl sulphoxide (DMSO) was added to each well. After shaking the plates for 20 minutes, the absorbance at 570 nm was measured with background subtraction at 655 nm. Each condition of treatment was performed at least in triplicate.

Trypan blue staining assay

Trypan blue staining assay was performed as reported [51]. Cells, plated in 6-well plates were exposed to differential treatments, harvested and stained with trypan blue reaction buffer (Sigma-Aldrich, USA) at the concentration of 0.4% for 20 min at room temperature. After that, cells were observed under a light microscope, and the dead blue cells were counted. The percentage of viable cells was calculated by using the following formula: cell viability (%) = (total cells-dead blue cells)/total cells × 100%.

Clonogenic survival assay

Cells were plated in triplicate into six-well plates and allowed to incubate for 8 days in the presence or absence of treatments. Then, the medium was removed and the cells were fixed using 4% paraformaldehyde (Sigma-Aldrich, USA) for 30 min fixed with methanol at room temperature for 15 min and stained with 1% crystal violet at room temperature for 30 min. Colonies consisting of >50 cells were counted.

TUNEL assay

Cells were exposed to treatments for 72 hours. Apoptosis was determined by enzymatic labeling of DNA strand breaks using terminal deoxynucleotidyl transferase-mediated deoxyuridine triphosphate nick end labeling, using APO-BrdUTM TUNEL Assay Kit (Promega, Madison, WI, USA).

Total RNA extraction, reverse transcription PCR and real-time RT-PCR assay

Total RNA was extracted from different cell types using TRIzol reagent and cDNA was synthesized by the reverse transcription-polymerase chain reaction (PCR) method using a RETROscript kit. Five microliters of diluted (1:4) cDNA was analyzed using SYBR Green Universal PCR Master Mix, following the manufacturer's recommendations. Real-time PCR was performed in the iCycler iQ Detection System (Bio-Rad, Milan, Italy), using 0.1 µM each primer in a total volume of 30 µL of reaction mixture following the manufacturer's recommendations. Each sample was normalized on the basis of its 18S ribosomal RNA content. The results were calculated and expressed as previously reported [52].

Immunoprecipitation and western blot

Cells were exposed to treatments for different times and processed to obtain cytoplasmic or total protein cell lysates. For immunoprecipitation studies, 500 µg of protein lysates were

incubated overnight with the specific antibody and processed as described [53]. Western blotting was performed as previously reported [54]. Autoradiographs show the results of one representative experiment out of three. Equal amount of protein extracts was subjected to SDS-PAGE. Images were acquired using Odissey FC (Licor, Lincoln, NB, USA). Numbers below the blots represent the average fold change versus control normalized for β-actin. Images are representative of three different experiments.

Transient transfection

Cells were transfected using the FuGENE 6 or Lipofectamine 2000 reagent (Invitrogen, Paisley, UK) as recommended by the manufacturer with a mixture containing specific constructs and then treated for different times as indicated.

Lipid-mediated transfection of siRNA duplexes

Cells were transfected with 4 functionally verified siRNA directed against human Beclin1 or with a control siRNA (Qiagen, Mi, Italy) that does not match with any human mRNA (Non-specific siRNA) for non-sequence specific effects. Cells were transfected using Lipofectamine 2000 reagent (Invitrogen, Paisley, UK) and then treated as indicated.

Flow cytometry

Cells, were serum starved for 18 hours and then treated with RSV and/or GSI for different times as indicated. To determine cell cycle distribution analysis, cells were harvested by trypsinization, fixed and stained with propidium iodide (100 μg/mL) after treatment with RNase A (20 μg/mL). The DNA content was measured using a FACS can flow cytometer (Becton Dickinson, Mountain View, CA, USA) and the data acquired using CellQuest software. Cell cycle profiles were determined using Mod-Fit LT.

GFP-LC3 fluorescence

LC3 translocation was detected using the green fluorescent protein (GFP)-fused LC3 construct (Cell Biolabs, Inc. San Diego, CA). Briefly, cells were seeded in 6 well plates contained glass coverslips and allowed to attach overnight. 7 μg of LC3-GFP expression plasmid were transfected using Fugene 6 reagent (Roche Diagnostics, Milan, Italy). Six hours after transfection, the cells were treated as indicated for 18 hours. The coverslips with attached cells were stained with the blue-fluorescent DAPI for nuclear stain. The excess buffer was removed and the coverslips were mounted. Fluorescence analysis was carried out on an OLYMPUS BX51 microscope. Images are representative of three different experiments. For manual quantification of the puncta, at least 3 optical fields per experimental condition were analyzed. Data from repeated experiments are subjected to statistical analysis.

FACS detection of acidic vesicular organelles

Acidic vesicular organelles (AVOs) were detected and quantified after vital staining with acridine orange to monitor autophagic phenotype [55]. Following treatment, cells were stained with 0.5 μg/ml acridine orange for 15 min at 37°C. Cells were then trypsinized and collected in phenol-red free medium. Green (510-530 nm) and red (>650 nm) fluorescence emission from cells was measured with a Fluorescence Activated Cell Sorter (FACS) using CellQuest software. The determination of Mean Red: Green Fluorescence Ratio in Acridine Orange-stained Cells Using Flow Cytometry was performed as previously reported [56].

Supravital cell-staining with acridine orange

Cell staining was performed according to published procedures [56]. Acridine orange (Sigma Chemical) was added at a final concentration of 1 mg/ml for 15 min. Pictures were obtained with a fluorescence OLYMPUS BX51 microscope. Images are representative of three different experiments.

Statistical analysis

The data were analyzed by one-way ANOVA using the GraphPad Prism 4 software program and the results were presented as mean ± SD. A value of $P \leq 0.05$ was considered to be significant.

Discussion

High grade gliomas are characterized by worse prognosis and treatment resistance. Although,

appropriate druggable target inhibition was possible in the initial stage of the tumor, the emergence of resistance leads to the progression of the disease [34]. The anti-tumor effect due to the inhibition of Notch, among different pathways, is reported in pre-clinical and *in vitro* studies [11, 13, 35]. Up to now it is emerging that Notch inhibition could be improved when used in conjunction with phytochemical compounds [36]. These combined approaches are often more effective over traditional single-agent therapy regimens for brain tumors, since the different drugs affect multiple pathways and cell clones. In such a way the therapeutic responses may be improved, dose and side effects reduced and drug resistance prevented [37]. Previous studies report the mechanism of RSV-mediated chemo-sensitization and its multifaceted efficacy in inhibiting the general pro-survival mechanisms [21, 38]. Our results validate the rationale of choosing the combination of a Notch inhibitor (GSI) and RSV, by demonstrating the efficacy of RSV in enhancing the signature events of autophagy/apoptosis switch in GBM experimental models. Therefore, the present research evidences the rise of the therapeutic efficacy of GSI, exploiting the combination with RSV. We demonstrated that the RSV and GSI work synergistically to prevent GBM cell proliferation through the autophagic flux inhibition and sustaining apoptosis transition. Importantly, we prove the crucial role of CDK4 inhibition due to RSV and GSI cotreatment which may lead to the autophagosome accumulation [30] and to the consequent pro-apoptotic impairment of the protein's digestion in the lysosome. This in turn, providing the block of metabolic intermediates that sustain cell growth and survival via downstream effectors, causes the switch towards apoptosis (**Figure 7**). The combination results in decreasing the IC50s to about 2.5-fold smaller for GSI and 4-fold smaller for RSV. Dose reduction of GSI, for given cytotoxicity effects, is clinically very important, since this may lead to less general side effects of the therapy.

Previous studies have shown that, the Notch receptors and components of the Notch signaling pathway governing glioma tumor development, are differently expressed in GBM tumors as well as in GBM-derived cultures [39]. Glioblastoma cell models, U87MG and T98G, show elevated Notch receptors expression compared with a human glial cell line. In these cells, RSV and GSI combination reduced the Notch1 receptor signal and the clonogenic potential, most likely as a consequence of the inhibitory effects on cell cycle phases progression. It should be considered that additional Notch downstream targets, other than HES1, could be of importance for the outcome of Notch activity in these cells. The cell cycle regulators p21 and cyclin D1 have been suggested as Notch targets [40]. CDK4 plays a fundamental role in drug resistance and pro-survival signals, besides amplification of CDK4 is reported in GBM samples [41]. Very recently, an elegant study demonstrated that CDK4 regulates lysosomal function and that CDK4 inhibition or depletion leads to the accumulation of intralysosomal undigested material [30]. Our results demonstrate, for the first time, that the inhibition of CDK4, by RSV and GSI combination, represents a fundamental molecular link for the block of the autophagic flux and the consequent switch through apoptosis. In our GBM cells, drugs combination induced the autophagy initiation but suppressed autophagic degradation, as evidenced by sustained LC3-II increase, suggesting the accumulation of autophagosomes. The autophagic flux disruption is due to CDK4 reduction and may cause the RSV+GSI cytotoxicity.

During efficient autophagy, macromolecules and organelles are degraded and recycled thus serving for different metabolic functions in cancer cells. Classically, LC3-I bound to phosphatidylethanolamine generates LC3-II [31], while the cargo adaptor protein p62/SQSTM1 binds to ubiquitinated proteins, transporting them to the phagophore, for subsequent degradation. In the meantime, p62/SQSTM1 itself is degraded by autolysosomes following the initiation of autophagy. Congruently, when autophagy is potently inhibited, p62/SQSTM1 accumulates in the cell. A study has reported that the p62/SQSTM1 accumulation is required for RSV-induced autophagic cell death in cancer cells [42]. We demonstrate that, the RSV+GSI cotreatment triggers the block of autophagic flux, evidenced by a sustained increase of LC3-II and p62/SQSTM1 accumulation, even though a certain acidic vesicular organelles formation is displayed in T98G cells. Taken together these results indicate that RSV and GSI combination can cause a block of the autophagic vesicles maturation process in glioblastoma cells.

The sustained increase of LC3-II and p62/SQSTM1, due to autophagosomes accumulation, is not accompanied by the functional upregulation of Beclin-1, an essential mediator for the formation and extension of pre-autophagosomal structure [31, 43, 44], addressing a Beclin-1 independent mechanism. In addition, we found, upon the combined treatment, the strong increase of Atg12, previously identified as an autophagic gene shared with the apoptotic pathways, in such way representing an important point of convergence between autophagy and apoptosis [45].

Autophagy and apoptosis are temporally tuned and frequently occur in an order in which autophagy leads to apoptosis [46]. It is known that the autophagy machinery can control cell death molecular events and the molecular mechanisms are only partially defined [47]. Bodies of evidence indicate that interruption of the late stage of autophagy drives an excessive accumulation of autophagosomes, which has the potential to turn autophagy into a destruction process inducing apoptosis [48]. This notion is strongly supported by our results, showing that apoptosis activation markers, such as caspase 3, caspase 9 and cleaved PARP, were particularly evident when cells were under the RSV and GSI synergism, while treatment with the single drug exerted only partial effects. Interestingly, apoptosis was evidenced but later than autophagy, as a consequence of the block of the autophagic flux, which is determinant for RSV+GSI-induced autophagic cell death. The early stage autophagy inhibitor 3-MA, dramatically reversed RSV+GSI induced caspases activation and apoptosis induction. Interestingly, it emerges how, the combined exposure to RSV+GSI leads to the described autophagosome accumulation and the subsequent apoptotic events. Among the multiple signaling pathways that have been generally implicated in GBM progression, the PTEN/PI3K/Akt/mTOR axis appears not substantially affected by RSV+GSI, while p42/p44MAPK was inhibited.

In summary, our study demonstrates that RSV+GSI cotreatment triggers apoptosis by pathways blocking the autophagic flux, through CDK4 inhibition, addressing how the Notch inhibitors and RSV combination could be prospectively implemented in the novel therapeutic strategy for GBM treatment.

Results

Resveratrol and a gamma secretase inhibitor exert synergistic cytotoxic effects in GBM cells

The abnormal expression of various Notch components in brain tumors correlates with a higher glioma grade and a worse prognosis, indicating that more activated Notch signaling promotes a more undifferentiated and aggressive tumor phenotype [6, 26, 27]. As shown in **Figure 1A**, in human GBM cells, U87MG and T98G, we observed that mRNA levels of the Notch Receptors (Notch1, Notch2 and Notch3) and HES1, a Notch direct target gene [28] were increased, much more than in the T47D breast cancer cells, with respect to human glial cell line (SVG p12), assumed as control. The mRNA levels of Notch4 were upregulated only in U87-MG cells. Next, we tested the effects produced by Resveratrol (RSV) and/or a gamma secretase inhibitor of Notch signaling, RO4929097 (GSI). Cotreatment with low doses of the drugs, 10 μM RSV and 2 μM GSI, produced a reduction of Notch1 and the transcriptionally active Notch1 intracellular domain (NICD) along with Notch target genes HES1 and HEY1 in both cell lines in terms of mRNA (**Figure 1B**) and/or protein levels (**Figure 1C**). To obtain evidence for the involvement of the cellular proteasome in RSV+GSI action, the effects of the MG132 proteosome inhibitor on Notch1 expression was examined (**Figure 1D**). Pretreatment with 100 nM MG132 was unable to reverse the RSV+GSI down-regulatory action of Notch1. Expression levels of Notch receptors 2, 3 and 4 were differently affected by co-treatment in the two cell lines tested (data not shown).

Cell viability assay was performed to evaluate the effects of RSV or GSI toward GBM cells. Both the compounds induced a dose-dependent cytotoxicity in the cell lines tested (**Figure 2A**). Next, various combinations of RSV plus GSI were evaluated (**Figure 2B**). A combination of 10 μM RSV and 2 μM GSI induced synergic cytotoxicity. The combinative index (CI) values, was 0.57 in the case of U87MG, whereas was 0,48 in T98G, thus both were <1, indicating the synergism in both cell lines. Interestingly, RSV and GSI combination effect is similar to the cytotoxicity induced by five times higher concentration of GSI alone. Further evaluation of the combination effects was obtained by Trypan blue assay and similar results were

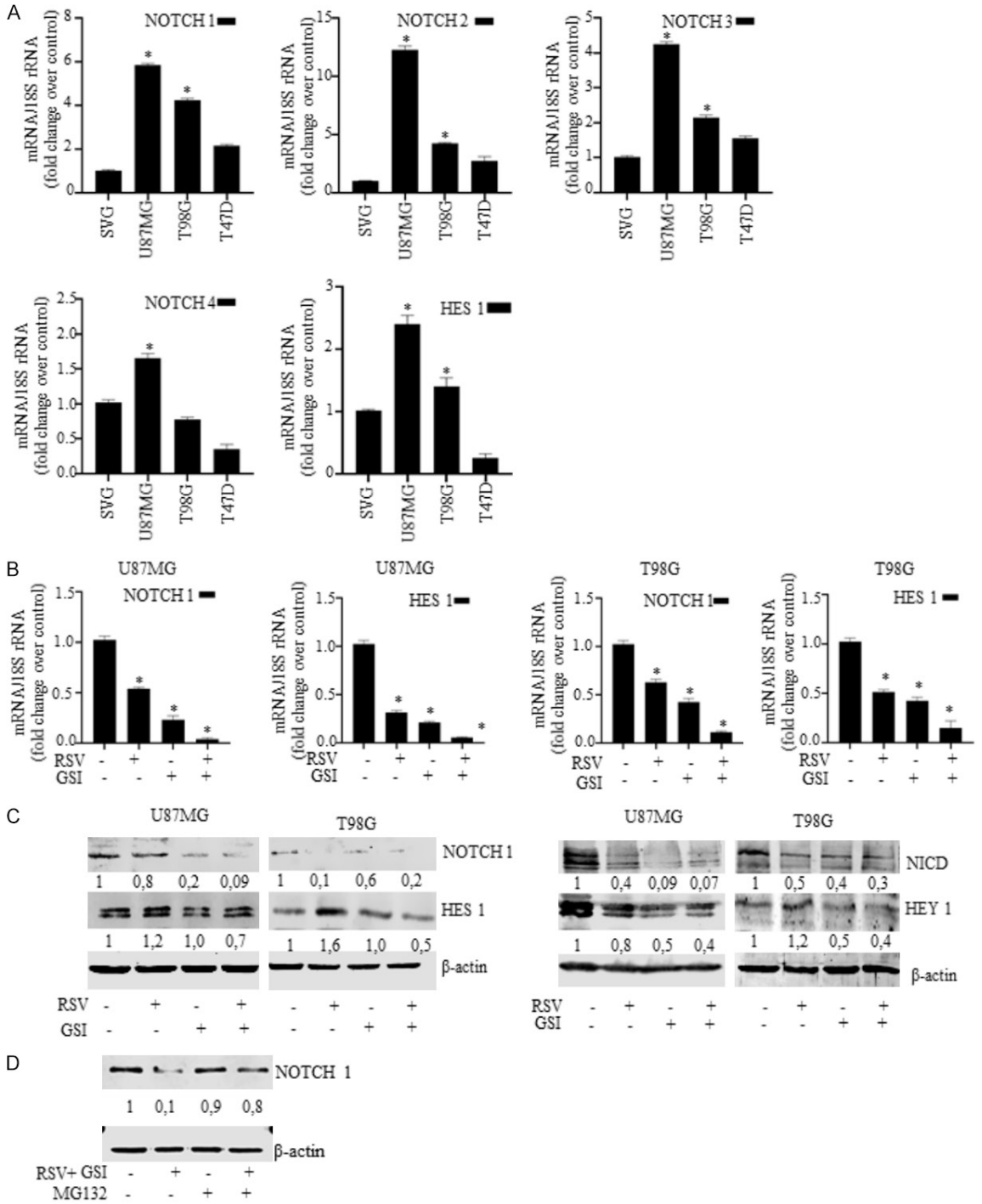

Figure 1. Resveratrol and GSI cotreatment reduces Notch1 and HES1 expression in GBM cells. A. Real-time PCR assay of Notch1, Notch2, Notch3, Notch4 and HES1 mRNA expression in different cell lines as indicated. Columns are the mean of three independent experiments each in triplicate; bars, SD; *P≤0.05 vs SVG cells. B. Real-time PCR assay of Notch1 and HES1 mRNA expression in U87MG and T98G cells treated with vehicle (-), 10 μM RSV and/or 2 μM GSI for 24 hours as indicated. 18S rRNA was determined as control. Columns are the mean of three independent experiments each in triplicate; bars, SD; *P≤0.05 vs vehicle. C. U87MG and T98G cells treated with vehicle (-), 10 μM RSV and/or 2 μM GSI for 24 hours as indicated and Western blot carried out for Notch1, HES1, NICD and HEY1 proteins. β actin was used as loading control. Autoradiograph shows the results of one representative experiment out of three. D. U87MG cells were pre-treated with MG132 for 2 h and then co-treated with 10 μM RSV plus 2 μM GSI for 24 h and Western blot carried out for Notch1.

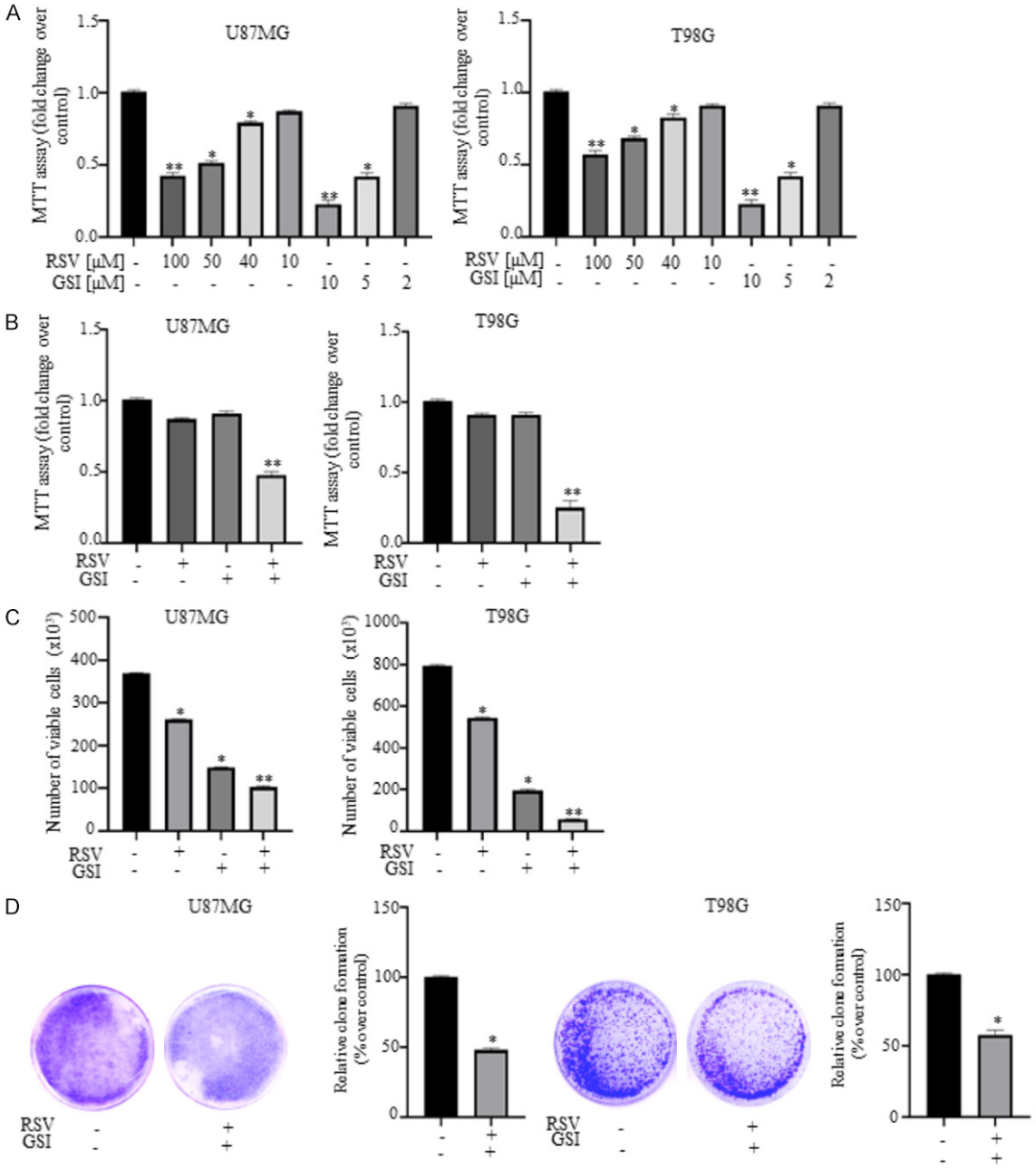

Figure 2. Resveratrol and GSI cotreatment reduces GBM cells viability. A. MTT assay. U87MG and T98G cells were treated for 48 hours with vehicle (-), or different concentrations of RSV or GSI as indicated. Columns are mean of three independent experiments and expressed as fold change over vehicle (control), which was assumed to be 1; bars, SD; *P≤0.05 vs vehicle. **P≤0.01 vs vehicle. B. MTT assay. U87MG and T98G cells were treated for 48 hours with vehicle (-), 10 μM RSV and/or 2 μM GSI as indicated. Columns are mean of three independent experiments; bars, SD; **P≤0.01 vs vehicle. C. Trypan bleu exclusion assay in U87MG and T98G cells treated for 72 hours with vehicle (-), 10 μM RSV and/or 2 μM GSI as indicated. Columns are mean of three independent experiments; bars, SD; *P≤0.05 vs vehicle; **P≤0.01 vs vehicle. D. Clonogenic survival assay in U87MG and T98G cells treated for 8 days with vehicle (-), or 10 μM RSV plus 2 μM GSI as indicated. Columns are mean of three independent experiments; bars, SD; *P≤0.05 vs vehicle. Images show the results of one representative experiment out of three.

observed (**Figure 2C**). The combination of RSV with GSI reduced also the clonogenic potential of U87MG and T98G cells (**Figure 2D**).

Alternative gamma secretase inhibitor, DAPT (N-[N-(3,5-difluorophenacetyl-L-alanyl)]-phenylglycinet-butyl ester) induced cytotoxic effects

(data not shown), but in a less extend, thus we used GSI for our next studies.

Distinct cell cycle effects of Resveratrol and a gamma secretase inhibitor in GBM cells

Glioblastoma cells were treated with RSV and/or GSI prior to flow cytometry. In U87MG, RSV induced a G1/S arrest, while GSI induced a G2/M arrest, after 48 hours (**Figure 3A**). Combined treatment, determined a marked reduction of the cell percentage in S phase but also in G1 phase, and more accumulated cells in the G2/M phase compared with the no-treatment control group, suggesting a G2/M arrest. We also evidenced a 7% of cells in the subG1 phase, indicating that the combined treatments lead to more apoptosis. Distinct drug responses features were displayed in T98G cells (**Figure 3B**) consistent with an enhanced percentage of the cells in G1 and G2 phases following the treatments with RSV and GSI, while the exposure to both drugs induced a marked rise in the percentage of cells in the subG1 (>14% cells). Since RSV and GSI cotreatment blocked the cell cycle progression in both cell types, we next examined whether these drugs could affect the expression of cell cycle regulatory proteins (**Figure 3C**). The most impressive events were represented by the decrease of the bridging molecule, cyclin D1 [29] in both cell lines after 48 hours of combined treatment. Moreover, we observed that, in U87MG cells, the cyclin D1 binding partner, CDK4 expression levels, were increased by GSI alone, which prompted us to evaluate the efficacy of RSV cotreatment in regulating it. Resveratrol cotreatment significantly reduced the basal and GSI induced expression of CDK4 in both GBM cell lines after 48 hours, thus we presumed a role of CDK4/cyclin D1 axis in the synergism.

Autophagy is an early and protective event induced by Resveratrol and a gamma secretase inhibitor in GBM cells

Beyond its role in cell cycle progression, CDK4 regulates lysosomal function [30], which is essential for autophagy, a conserved catabolic process that triggers the degradation of intracellular constituents and organelles in the lysosome [31]. When autophagy is activated, PI3KIII causes lipidation of LC3-I (microtubule-associated protein 1 light chain 3) which alters LC3-I electrophoretic mobility referred as LC3-II. LC3 I-II conversion was augmented by RSV and GSI combination, reaching the maximum value at 18/24 hours in both cell lines (**Figure 4A**) and maintained still after 48/72 hours (data not shown). Accordingly, RSV+GSI increased the GFP-LC3 puncta formation in U87MG cells with GFP-tagged LC3 transfection (**Figure 4B**). The ability of RSV and GSI to modulate the autophagic flux was next monitored by examining their combined effects on the expression of p62/SQSTM1, a commonly used indicator of the autophagic flux, since p62/SQSTM1 is itself degraded by autophagy. Our data show that cotreatment induced a sustained increase of p62/SQSTM1 protein content, time-dependently, in U87MG as well as in T98G cells (**Figure 4C**). These data suggest that drugs combination induced the block of the autophagic flux.

During the late stages of autophagy, autophagosomes fuse with lysosomes and the protein contents are degraded in the acidic environment of the organelle [31]. The presence of these acidic vesicular organelles (AVOs) can be detected by acridine orange staining and quantified by flow cytometry. To measure the cotreatment-induced effects in fractional volume and/or acidity of AVO, we determined the mean red: green fluorescence ratio in control and cotreated cells. While no significant effect was evident in U87MG, AVO appearance increased with the time after RSV and GSI combination in T98G cells (**Figure 4D**). Vital staining with acridine orange confirmed the appearance of AVO after cotreatment in T98G cells (**Figure 4E**). Given the results indicating the block of the autophagic flux, we thus hypothesized an impairment in the autophagic vesicles maturation process evoked by RSV+GSI in glioblastoma cells.

Next, we investigated the role of Beclin-1, an important autophagy effector that plays a key role in autophagosome formation [31]. The continuous time-dependent increase in LC3-II was inconsistent with the Beclin-1 amount fluctuations. Specifically, the expression of Beclin-1 does not showed noticeable changes in response to RSV+GSI treatment, at different times (**Figure 5A**). Beclin-1 downregulation using specific siRNA, confirmed that LC3 lipidation was not influenced by Beclin-1 expression levels (**Figure 5B**). Beclin-1/Bcl-2 interaction prevents Beclin-1 from assembling the pre-

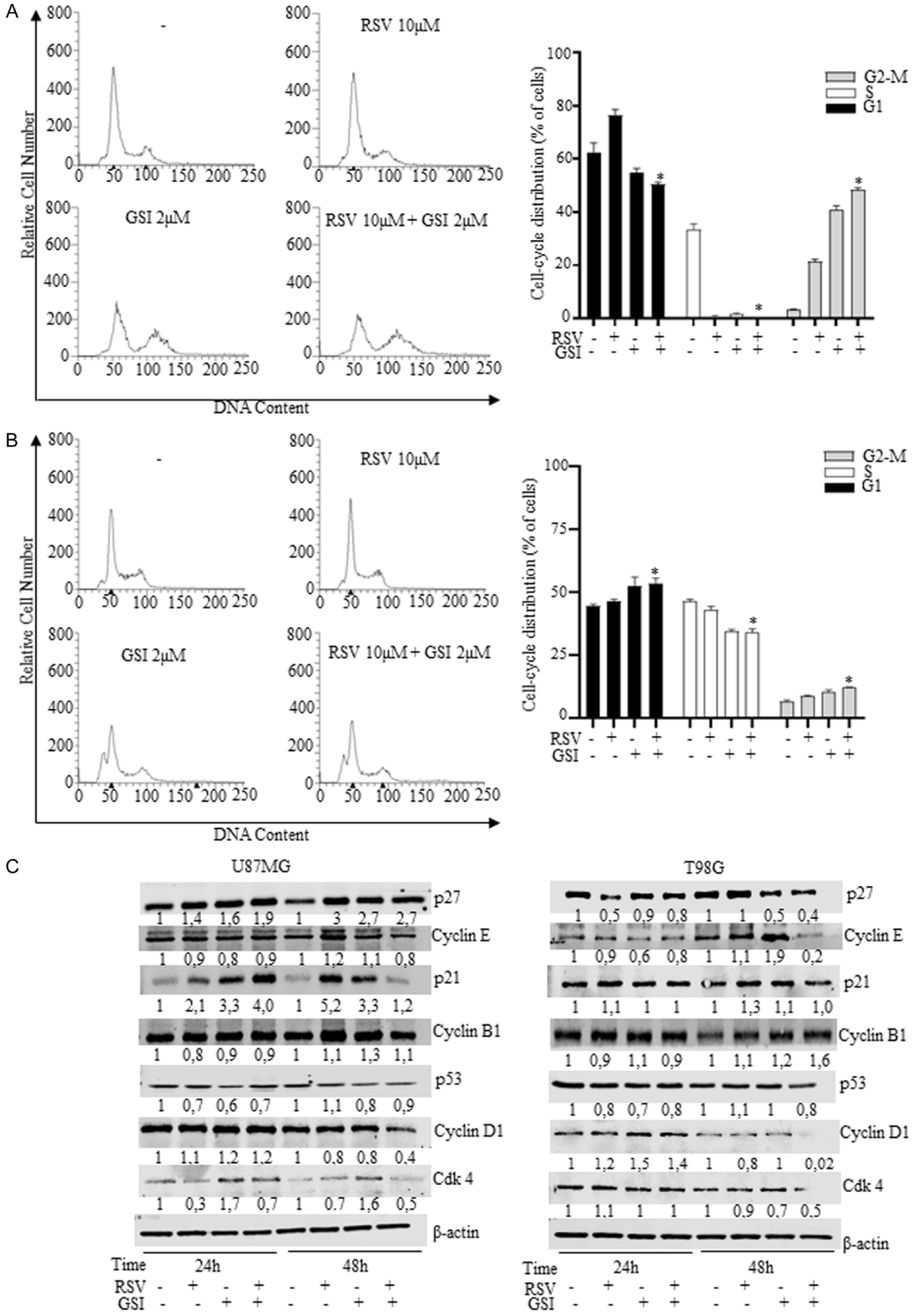

Figure 3. Effects of Resveratrol and GSI cotreatment on cell cycle phases distribution in GBM cells. (A) Cell cycle profile of U87MG and (B) T98G cells treated with vehicle (-) or 10 μM RSV and/or 2 μM GSI. Cells were stained with propidium iodide and analyzed using a FACS can flow cytometer. Images show the results of one representative ex-

periment out of three. In the right panels: quantitative analysis of percentage gated cells at G1, S and G2-M phases in the above reported experimental conditions. *P≤0.05 vs vehicle. (C) U87MG and T98G cells were treated with vehicle (-) or 10 μM RSV and/or 2 μM GSI for 24 and 48 hours, and Western blot carried out for the indicated proteins.

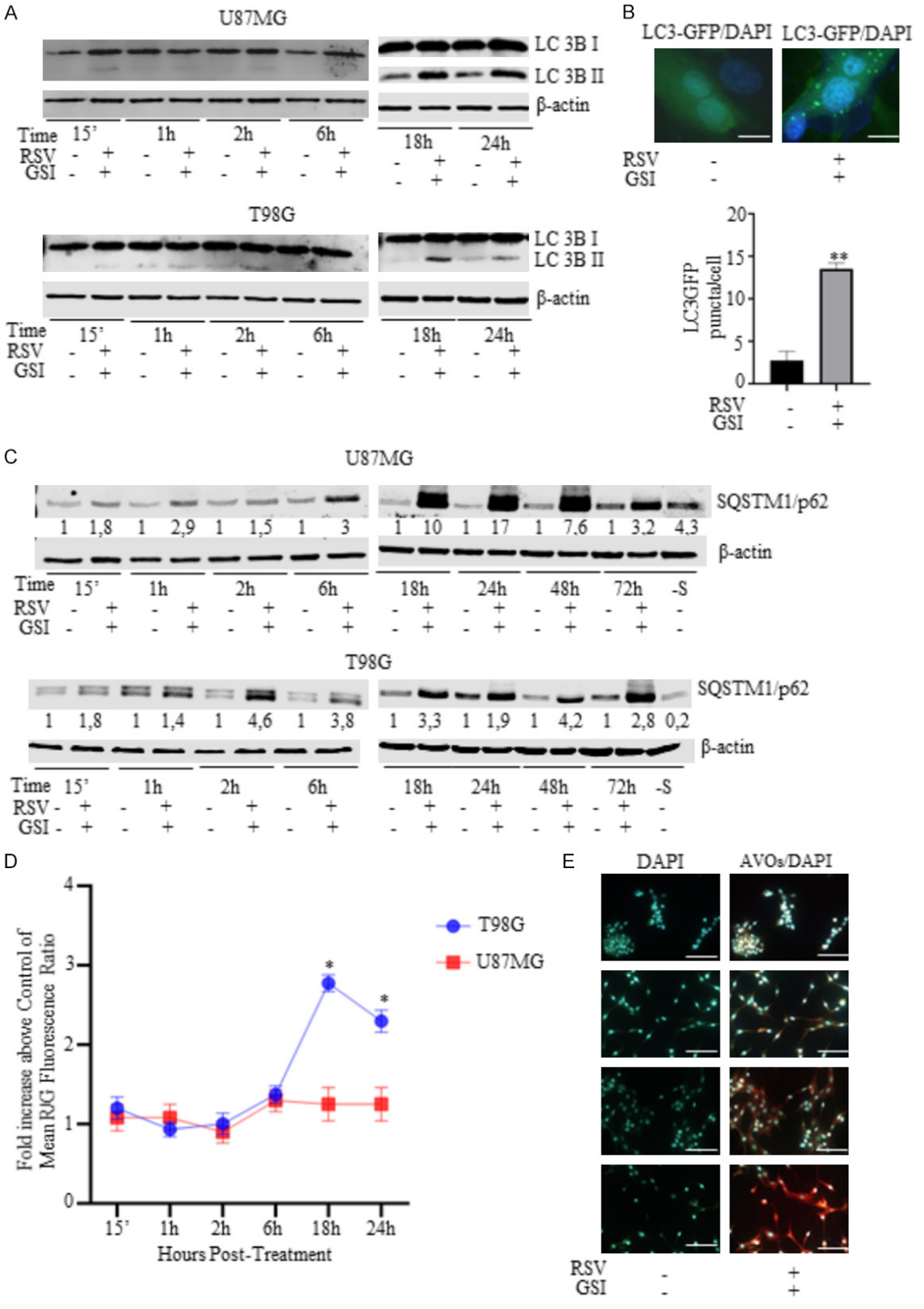

Figure 4. Resveratrol and GSI cotreatment induces the expression of autophagy markers in GBM cells. A. Time course study. U87MG and T98G cells were treated with vehicle (-) or 10 μM RSV plus 2 μM GSI for different times as indicated and Western blot carried out for LCI and LC3II. B. Upper panel. U87MG cells were transiently transfected with LC3-GFP and treated with vehicle (-) or 10 μM RSV plus 2 μM GSI for 18 hours. Images show the results of one representative experiment out of three. Scale bars = 5 μM. Lower panel, Number of LC3-GFP positive puncta manually counted in each of 50 cells/treatment. Data are means of three independent experiments. Columns are mean of three independent experiments. **P≤0.01 vs vehicle. C. Time course study. U87MG and T98G cells were treated with vehicle (-) or 10 μM RSV plus 2 μM GSI for different times as indicated and Western blot carried out for p62/SQSTM1. -S indicates cells maintained in absence of serum for 72 hours. D. Red:green (R/G) fluorescence ratio. U87MG and T98 cells were treated with vehicle (-) or 10 μM RSV plus 2 μM GSI for different times as indicated. Cells were stained and processed for flow cytometric analysis. The numbers represent the fold increase of the red: green fluorescence ratio in treated cells over vehicle controls, and are the mean of triplicate samples from one experiment that was reproduced twice with similar results. *P≤0.05 vs 15', vs 1 h, vs, 2 h, vs 6 h. E. Staining of T98G cells with acridine orange followed by fluorescence microscopy for appearance of AVO. Images show the results of one representative experiment out of three. DAPI staining was used to visualize the cell nucleus. Scale bars = 25 μM.

autophagosomal structure [31]. In untreated cells, Beclin-1 was associated with Bcl-2 and this association unchanged after cotreatment (**Figure 5C**). Accordingly, we assumed that the combination of RSV+GSI may induce a Beclin-1 independent autophagy in GBM cells. The conjugation between ATG12 and ATG5, is crucial for the phagophore elongation and the lipidation of LC3 during autophagy in mammalian cells [31]. Results of the western blot analysis showed a strong increase of ATG12 expression and of ATG12-ATG5 conjugate in T98G cells after drugs stimulus (**Figure 5D**), thus suggesting ATG12 dependent autophagy.

To interrogate the molecular link mediating the RSV+GSI induced biological effects in GBM cells we focused our attention on the CDK4 a major regulator of energy homeostasis. CDK4 decrease is crucial in the impairment of lysosomal function [30], thus, we hypothesized that the GSI and RSV combination effects on the autophagic flux could be critically made possible by CDK4 inhibition. The ectopic overexpression of the (R24C) CDK4 mutant, which abolishes the ability p16 (INK4a) to inhibit CDK4 [32], greatly counteracted the RSV+GSI induced increase of the autophagosome marker LC3-II, as compared with control cells (**Figure 5E**). These results suggest that the decrease of CDK4 expression impairs the lysosomal degradation steps which causes the block of the autophagic flux by RSV and GSI combination.

Thus, triggering autophagy in RSV+GSI-treated cells, which have impaired lysosomal function, could cause the collapse of the system and could result in cell death [33]. The pro-apoptotic signaling, MAPK p38 cascades was induced after cotreatment in both cell lines (**Figure 5F**) concomitantly the pro-survival MAPK p42/p44 signaling was inhibited, while PI3K-AKT-mTOR cascade only partially downregulated (data not shown). These results suggest that combined treatment causes a change in the balance between cell survival and cell death signals.

The synergistic effects of Resveratrol and a gamma secretase inhibitor are evidenced by the induction of apoptosis in GBM cells

Since our data demonstrate that RSV plus GSI cotreatment induces the block of the autophagic flux (**Figure 4**) in GBM cells, we investigated whether the accumulation of autophagosome could be determinant for cell death [33]. To this aim we used an inhibitor of autophagosome-lysosome fusion such as bafylomicin (Baf) and evaluated its effects on GBM cell growth, during cotreatment. Pretreatment with Baf, rescued the cytotoxic inhibitory effects of RSV+GSI (**Figure 6A**). Instead, treatment with 3 Methil Adenine (3MA), inhibitor of early autophagy targeting PI3K, as well as the ectopic overexpression of the (R24C) CDK4 mutant, effectively counteracted the apoptotic markers such as the increased degradation of apoptotic caspase, procaspase-3 and procaspase-9 in both cell lines, due to RSV and GSI combination (**Figure 6B**). These results strongly suggest that the inhibition of CDK4, responsible of impaired lysosomal function, represents a fundamental step for the molecular switch to apoptosis by RSV and GSI combination, through the block of the autophagic flux.

We next further investigated the correlation between the block of the autophagic flux, p38

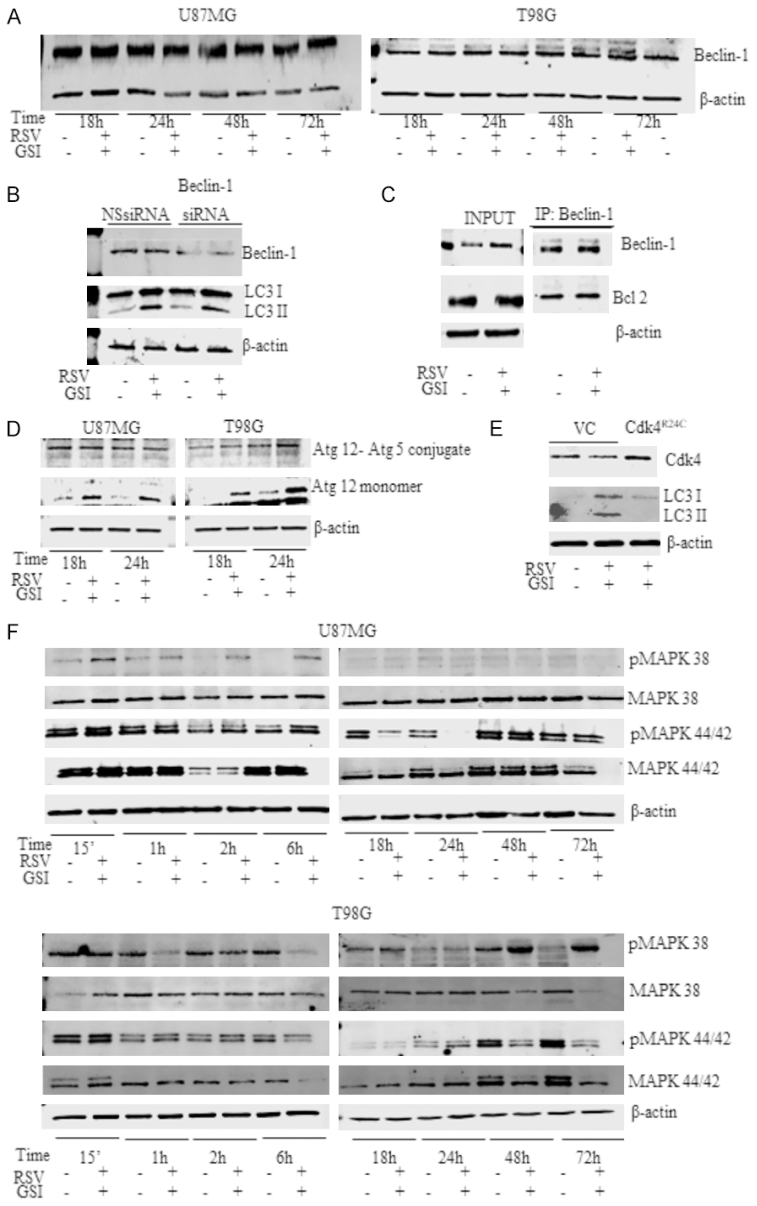

Figure 5. Resveratrol and GSI cotreatment changes the balance between pro-apoptotic and the pro-survival signaling in GBM cells. A. Time course study. U87MG and T98G cells were treated with vehicle (-) or 10 μM RSV plus 2 μM GSI for different times as indicated and Western blot carried out for Beclin-1. B. T98G cells transfected with non-specific siRNA (NS) or targeted against Beclin-1 siRNA, treated with vehicle (-) or 10 μM RSV plus 2 μM GSI for 24 hours and Western blot carried out for LCI and LC3II. C. Co-immunoprecipitation analysis. Total extracts from cells treated with vehicle (-) or RSV plus GSI for 24 hours, were used for INPUT or for immunoprecipitation (IP) by using specific anti-Beclin-1 antibody as indicated. Filters were blotted for the indicated proteins. D. U87MG and T98G cells were treated with vehicle (-) or 10 μM RSV plus 2 μM GSI for 18 hours and 24 hours and Western blot carried out for the indicated proteins. E. U87MG cells were transfected with vector control (VC) or R24C CDK4 mutant expression vector and treated for 24 hours as indicated. Western blot was carried out for CDK4, LC3I and LC3II. F. Time course study. U87MG and T98G cells were treated with vehicle (-) or 10 μM RSV plus 2 μM GSI for different times as indicated and Western blot carried out for the indicated proteins.

MAPK activation and the RSV+ GSI induced apoptosis. Increased degradation of procaspase-9, procaspase-8, procaspase-3 and PARP were observed in both cell lines after RSV and GSI combination in both cell lines (**Figure 6C**) as well as the up-regulation of the expression levels of the pro-apoptotic factor BAD (**Figure 6D**). These results provide evidences for apoptosis induction in RSV and GSI co-treated GBM cells, by possibly affecting caspase-associated pathways. Accordingly, we observed increased percentage of TUNEL positive cells, after 72 hrs of combined drugs addition (**Figure 6E**).

Together, these results demonstrate the role of CDK4 inhibition in the RSV and GSI triggered switch from autophagy to apoptosis in GBM cells (see **Figure 7**).

Acknowledgements

This work was supported by a special award (Department of Excellence, Italian Law 232/2016) from the Italian Ministry of Research and University (MIUR) to the Department of Pharmacy, Health and Nutritional Sciences of University of Calabria (Italy), by PON R&I FSE-FESR-2014-2020, by PON Salute ARS01_00568 PA.CRO.DE, by MIUR ex 60%.

Disclosure of conflict of interest

None.

Address correspondence to: Sebastiano Andò, Department of Pharmacy, Health and Nutritional Sciences, University of Calabria, Via P. Bucci, 87036, Rende (CS), Italy. E-mail: sebastiano.ando@

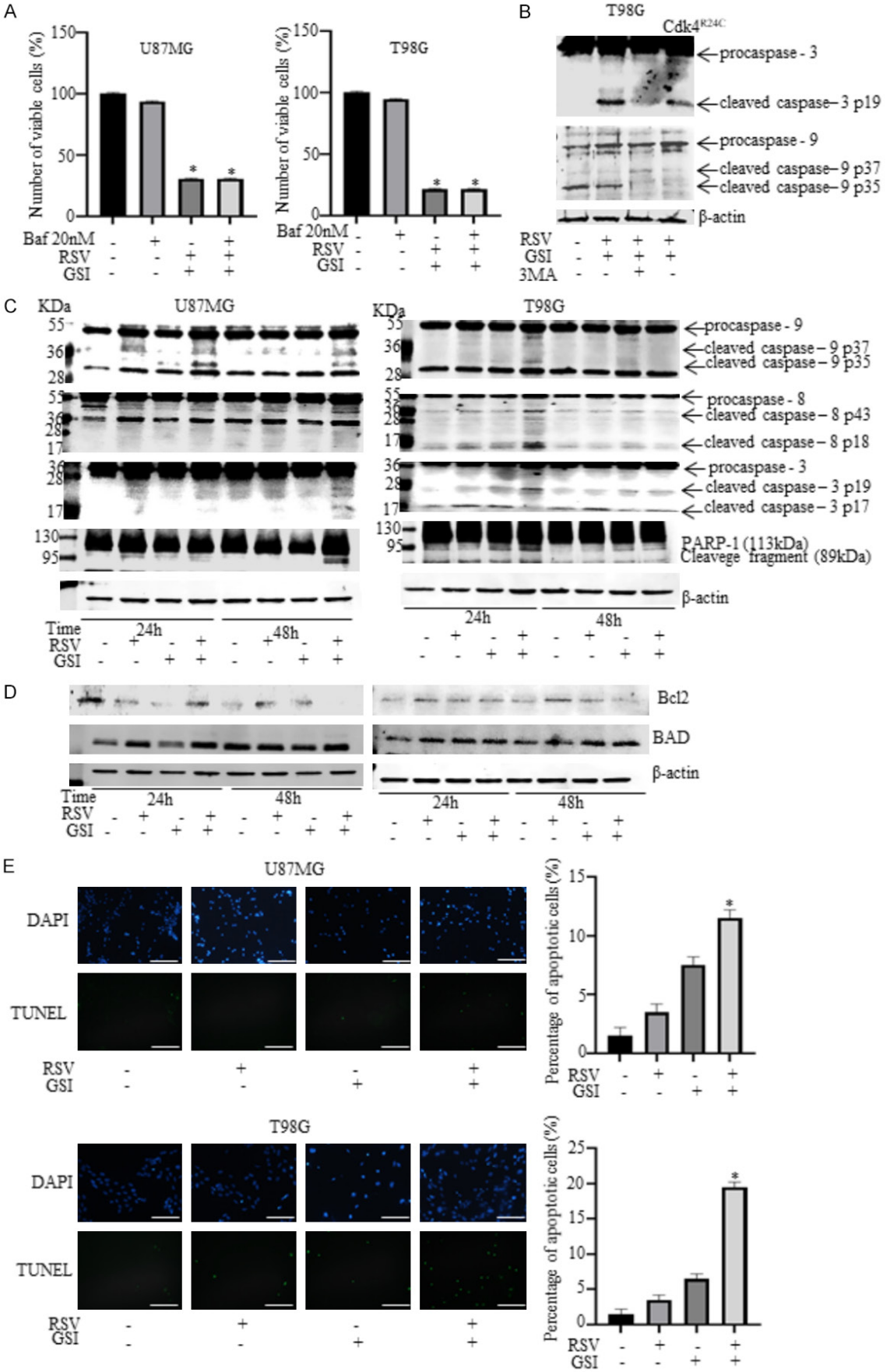
A
U87MG
T98G
Number of viable cells (%)
Baf 20nM
RSV
GSI
B
T98G
Cdk4R24C
procaspase - 3
cleaved caspase– 3 p19
procaspase - 9
cleaved caspase– 9 p37
cleaved caspase– 9 p35
β-actin
RSV
GSI
3MA
C
KDa
U87MG
T98G
procaspase - 9
cleaved caspase – 9 p37
cleaved caspase – 9 p35
procaspase - 8
cleaved caspase – 8 p43
cleaved caspase – 8 p18
procaspase - 3
cleaved caspase – 3 p19
cleaved caspase – 3 p17
PARP-1 (113kDa)
Cleavege fragment (89kDa)
β-actin
Time
24h
48h
RSV
GSI
D
Bcl2
BAD
β-actin
Time
24h
48h
RSV
GSI
E
U87MG
DAPI
TUNEL
RSV
GSI
Percentage of apoptotic cells (%)
T98G
DAPI
TUNEL
RSV
GSI
Percentage of apoptotic cells (%)

Figure 6. Resveratrol and/ GSI cotreatment induces apoptosis in GBM cells. A. Trypan bleu exclusion assay. U87MG cells were treated with vehicle (-), or 10 μM RSV and 2 μM GSI for 72 hours as indicated, in the presence or absence of Bafilomycin (Baf) pretreatment. Columns are mean of three independent experiments. *P≤0.05 vs vehicle. B. T98G cells were transfected with vector control (VC) or R24C CDK4 mutant expression vector and treated with vehicle (-) or 5 mM 3Methil Adenin (3MA) and/or 10 μM RSV+2 μM GSI as indicated for 48 hours, and Western blot carried out for the indicated proteins. C, D. U87MG and T98G cells were treated with vehicle (-) or 10 μM RSV and/ or 2 μM GSI for 24 and 48 hours, and Western blot carried out for the indicated proteins. E. TUNEL assay. U87MG and T98G cells treated with vehicle (-) or 10 μM RSV and/or 2 μM GSI as indicated for 72 hours. DAPI staining was used to visualize the cell nucleus. Scale bars = 25 μm. In the diagrams are represented the quantification of TUNEL staining images, as the average of apoptotic cells. Columns are mean of three independent experiments. *P≤0.05 vs vehicle, vs RSV, vs GSI.

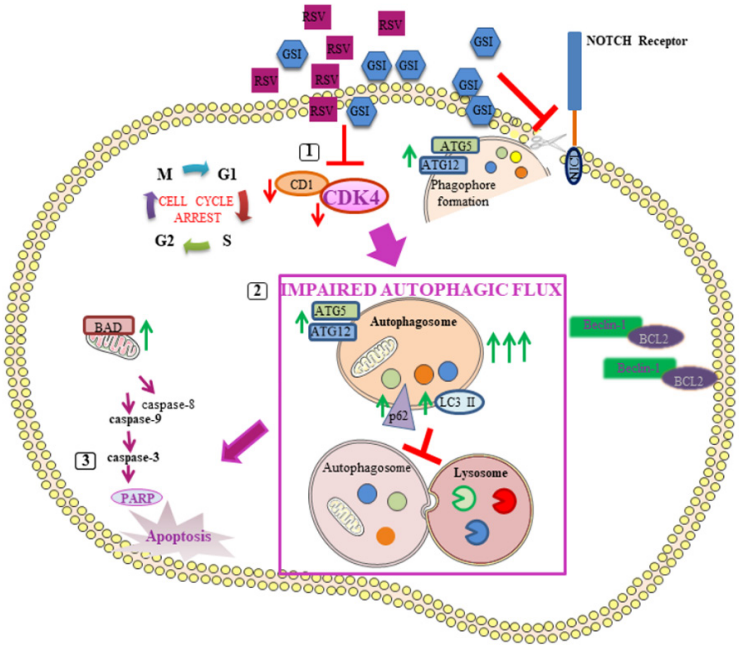

Figure 7. Proposed model for RSV+GSI-induced autophagy-apoptosis switch in GBM cells. A schematic summary illustrating CDK4 as a key target of RSV plus GSI combined treatment in GBM cells. 1) RSV plus GSI reduce CDK4/Cyclin D1 levels. 2) CDK4 inhibition is responsible of the IMPAIRED AUTOPHAGIC FLUX, the sustained increase of LC3-II and p62/SQSTM1 accumulation 3) The IMPAIRED AUTOPHAGIC FLUX, providing the block of metabolic intermediates that fuel cell growth and survival, causes the switch towards apoptosis. See the text for details. Abbreviations: ATG5: Autophagy related 5; ATG12: Autophagy related 12; BAD: BCL2 associated agonist of cell death; BCL-2: B-cell lymphoma 2; CDK4: cyclin-dependent kinase 4; GSI: RO4929097; LC3-II: LC3-phosphatidylethanolamine conjugate; NICD: Notch receptor intracellular domain; p62: ubiquitin-binding protein p62; PARP: Poly (ADP-ribose) polymerase; RSV: Resveratrol.

unical.it; Francesca De Amicis, Department of Pharmacy, Health and Nutritional Sciences, University of Calabria, Via P. Bucci, 87036, Rende (CS), Italy. E-mail: francesca.deamicis@unical.it

References

[1] Lee E, Yong RL, Paddison P and Zhu J. Comparison of glioblastoma (GBM) molecular classification methods. Semin Cancer Biol 2018; 53: 201-211.

[2] Le Rhun E, Preusser M, Roth P, Reardon DA, van den Bent M, Wen P, Reifenberger G and Weller M. Molecular targeted therapy of glioblastoma. Cancer Treat Rev 2019; 80: 101896.

[3] Weller M, Butowski N, Tran DD, Recht LD, Lim M, Hirte H, Ashby L, Mechtler L, Goldlust SA, Iwamoto F, Drappatz J, O'Rourke DM, Wong M, Hamilton MG, Finocchiaro G, Perry J, Wick W, Green J, He Y, Turner CD, Yellin MJ, Keler T, Davis TA, Stupp R and Sampson JH; ACT IV trial investigators. Rindopepimut with temozolomide for patients with newly diagnosed, EGFRvIII-expressing glioblastoma (ACT IV): a randomised, double-blind, international phase 3 trial. Lancet Oncol 2017; 18: 1373-1385.

[4] Ohgaki H and Kleihues P. Genetic alterations and signaling pathways in the evolution of gliomas. Cancer Sci 2009; 100: 2235-2241.

[5] Bazzoni R and Bentivegna A. Role of Notch signaling pathway in glioblastoma pathogenesis. Cancers (Basel) 2019; 11: 292.

[6] Purow BW, Haque RM, Noel MW, Su Q, Burdick MJ, Lee J, Sundaresan T, Pastorino S, Park JK, Mikolaenko I, Maric D, Eberhart CG and Fine HA. Expression of Notch-1 and its ligands, Delta-like-1 and Jagged-1, is critical for glioma cell survival and proliferation. Cancer Res 2005; 65: 2353-2363.

[7] Natsumeda M, Maitani K, Liu Y, Miyahara H, Kaur H, Chu Q, Zhang H, Kahlert UD and Eberhart CG. Targeting Notch signaling and autophagy increases cytotoxicity in glioblastoma neurospheres. Brain Pathol 2016; 26: 713-723.

[8] Purow B. Notch inhibition as a promising new approach to cancer therapy. Adv Exp Med Biol 2012; 727: 305-319.
[9] Luistro L, He W, Smith M, Packman K, Vilenchik M, Carvajal D, Roberts J, Cai J, Berkofsky-Fessler W, Hilton H, Linn M, Flohr A, Jakob-Rotne R, Jacobsen H, Glenn K, Heimbrook D and Boylan JF. Preclinical profile of a potent gamma-secretase inhibitor targeting Notch signaling with in vivo efficacy and pharmacodynamic properties. Cancer Res 2009; 69: 7672-7680.
[10] Guo H, Lu Y, Wang J, Liu X, Keller ET, Liu Q, Zhou Q and Zhang J. Targeting the Notch signaling pathway in cancer therapeutics. Thorac Cancer 2014; 5: 473-486.
[11] Xu R, Shimizu F, Hovinga K, Beal K, Karimi S, Droms L, Peck KK, Gutin P, Iorgulescu JB, Kaley T, DeAngelis L, Pentsova E, Nolan C, Grommes C, Chan T, Bobrow D, Hormigo A, Cross JR, Wu N, Takebe N, Panageas K, Ivy P, Supko JG, Tabar V and Omuro A. Molecular and clinical effects of Notch inhibition in glioma patients: a phase 0/I trial. Clin Cancer Res 2016; 22: 4786-4796.
[12] Samon JB, Castillo-Martin M, Hadler M, Ambesi-Impiobato A, Paietta E, Racevskis J, Wiernik PH, Rowe JM, Jakubczak J, Randolph S, Cordon-Cardo C and Ferrando AA. Preclinical analysis of the gamma-secretase inhibitor PF-03084014 in combination with glucocorticoids in T-cell acute lymphoblastic leukemia. Mol Cancer Ther 2012; 11: 1565-1575.
[13] Peereboom DM, Ye X, Mikkelsen T, Lesser GJ, Lieberman FS, Robins HI, Ahluwalia MS, Sloan AE and Grossman SA. A phase II and pharmacodynamic Trial of R04929097 for patients with recurrent/progressive glioblastoma. Neurosurgery 2021; 88: 246-251.
[14] Milano J, McKay J, Dagenais C, Foster-Brown L, Pognan F, Gadient R, Jacobs RT, Zacco A, Greenberg B and Ciaccio PJ. Modulation of Notch processing by gamma-secretase inhibitors causes intestinal goblet cell metaplasia and induction of genes known to specify gut secretory lineage differentiation. Toxicol Sci 2004; 82: 341-358.
[15] Riccio O, van Gijn ME, Bezdek AC, Pellegrinet L, van Es JH, Zimber-Strobl U, Strobl LJ, Honjo T, Clevers H and Radtke F. Loss of intestinal crypt progenitor cells owing to inactivation of both Notch1 and Notch2 is accompanied by derepression of CDK inhibitors p27Kip1 and p57Kip2. EMBO Rep 2008; 9: 377-383.
[16] De Amicis F, Chimento A, Montalto FI, Casaburi I, Sirianni R and Pezzi V. Steroid receptor signallings as targets for Resveratrol actions in breast and prostate cancer. Int J Mol Sci 2019; 20: 1087.
[17] Conte A, Kisslinger A, Procaccini C, Paladino S, Oliviero O, de Amicis F, Faicchia D, Fasano D, Caputo M, Matarese G, Pierantoni GM and Tramontano D. Convergent effects of Resveratrol and PYK2 on prostate cells. Int J Mol Sci 2016; 17: 1542.
[18] Carter LG, D'Orazio JA and Pearson KJ. Resveratrol and cancer: focus on in vivo evidence. Endocr Relat Cancer 2014; 21: R209-225.
[19] Wang Q, Xu J, Rottinghaus GE, Simonyi A, Lubahn D, Sun GY and Sun AY. Resveratrol protects against global cerebral ischemic injury in gerbils. Brain Res 2002; 958: 439-447.
[20] Zhang S, Botchway BOA, Zhang Y and Liu X. Resveratrol can inhibit Notch signaling pathway to improve spinal cord injury. Ann Anat 2019; 223: 100-107.
[21] De Amicis F, Giordano F, Vivacqua A, Pellegrino M, Panno ML, Tramontano D, Fuqua SA and Ando S. Resveratrol, through NF-Y/p53/Sin3/HDAC1 complex phosphorylation, inhibits estrogen receptor alpha gene expression via p38MAPK/CK2 signaling in human breast cancer cells. FASEB J 2011; 25: 3695-3707.
[22] Conte A, Procaccini C, Iannelli P, Kisslinger A, De Amicis F, Pierantoni GM, Mancini FP, Matarese G and Tramontano D. Effects of Resveratrol on p66Shc phosphorylation in cultured prostate cells. Transl Med UniSa 2015; 13: 47-58.
[23] Yuan Y, Xue X, Guo RB, Sun XL and Hu G. Resveratrol enhances the antitumor effects of temozolomide in glioblastoma via ROS-dependent AMPK-TSC-mTOR signaling pathway. CNS Neurosci Ther 2012; 18: 536-546.
[24] Huang H, Lin H, Zhang X and Li J. Resveratrol reverses temozolomide resistance by down-regulation of MGMT in T98G glioblastoma cells by the NF-kappaB-dependent pathway. Oncol Rep 2012; 27: 2050-2056.
[25] Sun Z, Li H, Shu XH, Shi H, Chen XY, Kong QY, Wu ML and Liu J. Distinct sulfonation activities in Resveratrol-sensitive and Resveratrol-insensitive human glioblastoma cells. FEBS J 2012; 279: 2381-2392.
[26] Teodorczyk M and Schmidt MHH. Notching on cancer's door: Notch signaling in brain tumors. Front Oncol 2014; 4: 341.
[27] Kanamori M, Kawaguchi T, Nigro JM, Feuerstein BG, Berger MS, Miele L and Pieper RO. Contribution of Notch signaling activation to human glioblastoma multiforme. J Neurosurg 2007; 106: 417-427.
[28] Monahan P, Rybak S and Raetzman LT. The Notch target gene HES1 regulates cell cycle inhibitor expression in the developing pituitary. Endocrinology 2009; 150: 4386-4394.

[29] Montalto FI and De Amicis F. Cyclin D1 in cancer: a molecular connection for cell cycle control, adhesion and invasion in tumor and stroma. Cells 2020; 9: 2648.
[30] Martinez-Carreres L, Puyal J, Leal-Esteban LC, Orpinell M, Castillo-Armengol J, Giralt A, Dergai O, Moret C, Barquissau V, Nasrallah A, Pabois A, Zhang L, Romero P, Lopez-Mejia IC and Fajas L. CDK4 regulates lysosomal function and mtorc1 activation to promote cancer cell survival. Cancer Res 2019; 79: 5245-5259.
[31] Wen X and Klionsky DJ. At a glance: a history of autophagy and cancer. Semin Cancer Biol 2020; 66: 3-11.
[32] Rane SG, Cosenza SC, Mettus RV and Reddy EP. Germ line transmission of the Cdk4(R24C) mutation facilitates tumorigenesis and escape from cellular senescence. Mol Cell Biol 2002; 22: 644-656.
[33] Button RW, Roberts SL, Willis TL, Hanemann CO and Luo S. Accumulation of autophagosomes confers cytotoxicity. J Biol Chem 2017; 292: 13599-13614.
[34] Qazi MA, Vora P, Venugopal C, Sidhu SS, Moffat J, Swanton C and Singh SK. Intratumoral heterogeneity: pathways to treatment resistance and relapse in human glioblastoma. Ann Oncol 2017; 28: 1448-1456.
[35] Moore G, Annett S, McClements L and Robson T. Top Notch targeting strategies in cancer: a detailed overview of recent insights and current perspectives. Cells 2020; 9: 1503.
[36] Vengoji R, Macha MA, Batra SK and Shonka NA. Natural products: a hope for glioblastoma patients. Oncotarget 2018; 9: 22194-22219.
[37] Bijnsdorp IV, Giovannetti E and Peters GJ. Analysis of drug interactions. Methods Mol Biol 2011; 731: 421-434.
[38] Gupta SC, Kannappan R, Reuter S, Kim JH and Aggarwal BB. Chemosensitization of tumors by Resveratrol. Ann N Y Acad Sci 2011; 1215: 150-160.
[39] Xing ZY, Sun LG and Guo WJ. Elevated expression of Notch-1 and EGFR induced apoptosis in glioblastoma multiforme patients. Clin Neurol Neurosurg 2015; 131: 54-58.
[40] Guo D, Ye J, Dai J, Li L, Chen F, Ma D and Ji C. Notch-1 regulates Akt signaling pathway and the expression of cell cycle regulatory proteins cyclin D1, CDK2 and p21 in T-ALL cell lines. Leuk Res 2009; 33: 678-685.
[41] Brennan CW, Verhaak RG, McKenna A, Campos B, Noushmehr H, Salama SR, Zheng S, Chakravarty D, Sanborn JZ, Berman SH, Beroukhim R, Bernard B, Wu CJ, Genovese G, Shmulevich I, Barnholtz-Sloan J, Zou L, Vegesna R, Shukla SA, Ciriello G, Yung WK, Zhang W, Sougnez C, Mikkelsen T, Aldape K, Bigner DD, Van Meir EG, Prados M, Sloan A, Black KL, Eschbacher J, Finocchiaro G, Friedman W, Andrews DW, Guha A, Iacocca M, O'Neill BP, Foltz G, Myers J, Weisenberger DJ, Penny R, Kucherlapati R, Perou CM, Hayes DN, Gibbs R, Marra M, Mills GB, Lander E, Spellman P, Wilson R, Sander C, Weinstein J, Meyerson M, Gabriel S, Laird PW, Haussler D, Getz G, Chin L and Network TR. The somatic genomic landscape of glioblastoma. Cell 2013; 155: 462-477.
[42] Puissant A, Robert G, Fenouille N, Luciano F, Cassuto JP, Raynaud S and Auberger P. Resveratrol promotes autophagic cell death in chronic myelogenous leukemia cells via JNK-mediated p62/SQSTM1 expression and AMPK activation. Cancer Res 2010; 70: 1042-1052.
[43] De Amicis F, Guido C, Santoro M, Giordano F, Dona A, Rizza P, Pellegrino M, Perrotta I, Bonofiglio D, Sisci D, Panno ML, Tramontano D, Aquila S and Ando S. Ligand activated progesterone receptor B drives autophagy-senescence transition through a Beclin-1/Bcl-2 dependent mechanism in human breast cancer cells. Oncotarget 2016; 7: 57955-57969.
[44] Pattingre S, Tassa A, Qu X, Garuti R, Liang XH, Mizushima N, Packer M, Schneider MD and Levine B. Bcl-2 antiapoptotic proteins inhibit Beclin 1-dependent autophagy. Cell 2005; 122: 927-939.
[45] Rubinstein AD, Eisenstein M, Ber Y, Bialik S and Kimchi A. The autophagy protein Atg12 associates with antiapoptotic Bcl-2 family members to promote mitochondrial apoptosis. Mol Cell 2011; 44: 698-709.
[46] Maiuri MC, Zalckvar E, Kimchi A and Kroemer G. Self-eating and self-killing: crosstalk between autophagy and apoptosis. Nat Rev Mol Cell Biol 2007; 8: 741-752.
[47] Denton D, Nicolson S and Kumar S. Cell death by autophagy: facts and apparent artefacts. Cell Death Differ 2012; 19: 87-95.
[48] Pan H, Wang Y, Na K, Wang Y, Wang L, Li Z, Guo C, Guo D and Wang X. Autophagic flux disruption contributes to Ganoderma lucidum polysaccharide-induced apoptosis in human colorectal cancer cells via MAPK/ERK activation. Cell Death Dis 2019; 10: 456.
[49] Santoro M, Guido C, De Amicis F, Sisci D, Cione E, Vincenza D, Dona A, Panno ML and Aquila S. Bergapten induces metabolic reprogramming in breast cancer cells. Oncol Rep 2016; 35: 568-576.
[50] Rovito D, Gionfriddo G, Barone I, Giordano C, Grande F, De Amicis F, Lanzino M, Catalano S, Ando S and Bonofiglio D. Ligand-activated PPARgamma downregulates CXCR4 gene expression through a novel identified PPAR response element and inhibits breast cancer progression. Oncotarget 2016; 7: 65109-65124.

[51] De Amicis F, Chiodo C, Morelli C, Casaburi I, Marsico S, Bruno R, Sisci D, Ando S and Lanzino M. AIB1 sequestration by androgen receptor inhibits estrogen-dependent cyclin D1 expression in breast cancer cells. BMC Cancer 2019; 19: 1038.

[52] Montalto FI, Giordano F, Chiodo C, Marsico S, Mauro L, Sisci D, Aquila S, Lanzino M, Panno ML, Ando S and De Amicis F. Progesterone receptor B signaling reduces breast cancer cell aggressiveness: role of Cyclin-D1/Cdk4 mediating Paxillin phosphorylation. Cancers (Basel) 2019; 11: 1201.

[53] de Amicis F, Lanzino M, Kisslinger A, Cali G, Chieffi P, Ando S, Mancini FP and Tramontano D. Loss of proline-rich tyrosine kinase 2 function induces spreading and motility of epithelial prostate cells. J Cell Physiol 2006; 209: 74-80.

[54] Mauro L, Sisci D, Bartucci M, Salerno M, Kim J, Tam T, Guvakova MA, Ando S and Surmacz E. SHC-alpha5beta1 integrin interactions regulate breast cancer cell adhesion and motility. Exp Cell Res 1999; 252: 439-448.

[55] De Amicis F, Guido C, Santoro M, Lanzino M, Panza S, Avena P, Panno ML, Perrotta I, Aquila S and Ando S. A novel functional interplay between Progesterone Receptor-B and PTEN, via AKT, modulates autophagy in breast cancer cells. J Cell Mol Med 2014; 18: 2252-2265.

[56] Paglin S, Hollister T, Delohery T, Hackett N, McMahill M, Sphicas E, Domingo D and Yahalom J. A novel response of cancer cells to radiation involves autophagy and formation of acidic vesicles. Cancer Res 2001; 61: 439-444.